Materials Research Proceedings **8** (2018) 88-88 doi: http://dx.doi.org/10.21741/9781945291999-9

Caracterisation of high manganese silicides prepared by mechanical milling

Victor CEBOTARI[1, a], Florin POPA[1, b], Traian Florin MARINCA[1, c], Violeta POPESCU[2, d], Ionel CHICINAŞ[1, e,*]

[1]Materials Science and Engineering Department, Technical University of Cluj-Napoca, 103-105, Muncii Avenue, 400641 Cluj-Napoca, Romania

[2]Physics and Chemistry Department, Technical University of Cluj-Napoca, 103-105, Muncii Avenue, 400641 Cluj-Napoca, România

[a]Victor.Cebotari@stm.utcluj.ro, [b]Florin.Popa@stm.utcluj.ro, [c]Traian.Marinca@stm.utcluj.ro, [d]Violeta.Popescu@chem.utcluj.ro, [e]Ionel.Chicinas@stm.utcluj.ro

Keywords: Thermoelectric, Higher Manganese Silicide, MnSi phase, Mechanical Alloying.

Abstract. The mechanical milling of manganese and silicon powder in a planetary ball mill up to 18 h was performed. In the X-ray diffraction pattern recorded after 18 hours of milling the MnSi phase and $Mn_{15}Si_{26}$ compound are detected. The agglomeration of powders after complete reaction of the elements was observed by scanning electron microscopy. Heating up at 1000 °C, an unreacted sample, milled 4 hours, has found to have the effect of completing the reaction of elements, but forms oxides. Handling of the powder during sampling, without protective atmosphere was found to form oxides. The oxidation of the samples was evidenced by FTIR analysis.

Introduction

The modern society has the tendency to increase the quantity of hydrocarbons which are transformed into energy, with negative effects on the environment. To reduce this impact alternatives are searched. Thermoelectric materials represent a solution to improve the quality of the environment by reducing the combustion product gases. These materials are able to convert the thermal energy directly into electrical energy and vice versa. The quality of a thermoelectric material can be estimated by the figure of merit $ZT=S^2\sigma T/k$ where: S is the Seebeck coefficient, σ is electrical conductivity, T is temperature and k is thermal conductivity [1]. Thermoelectric materials can convert heat from a different source such as solar heat, geothermal heat or exhaust gases [2]. From the studied thermoelectric materials, those based on silicon, especially High Manganese Silicide (HMS) is friendly with the environment and considered as promising candidates. HMS is chemically stable [3] and are preferred in detriment of those based on Pb-Te which operate in the same range of temperature. The HMS materials are nontoxic as well as their constituent chemical elements [4].

HMS are thermoelectric compounds with p-type conduction, having general formula $MnSi_x$ where the x value ranges from 1.67 up to 1.87 [5] and with an energy gap of 0.77 [eV] [6]. HMS system contains four compounds, Mn_4Si_7, $Mn_{11}Si_{19}$, $Mn_{15}Si_{26}$, and $Mn_{27}Si_{47}$, all with the same electronic structure [7]. Crystallographic structure of HMS compounds belongs to Nowotny chimney ladder (NCL) phases, where manganese is located in the corners of tetragon and silicon are arranged inside in the form of a spiral [8]. $MnSi_{1.75}$ compound presents the largest ZT, while the $MnSi_{1.77}$ compound has the smallest value. The low value for the figure of merit is the effect of

Materials Research Proceedings **8** (2018) 88-88 doi: http://dx.doi.org/10.21741/9781945291999-9

a large thermal conductivity [6]. Problem with HMS is that obtaining method influence the final phase. Based on the preparation method it is possible to obtain different compounds: by vacuum levitation melting $Mn_{15}Si_{26}$ is obtained, Mn_4Si_7 may obtain by vacuum levitation-induction melting and by dry milling [9-11]. Preparation by melting leads to an inhomogeneous structure and coarse microstructure [12]. The obtaining by mechanical alloying has the advantage of obtaining a small crystallite size which leads to lower thermal conductivity [11]. Also, dry milling leads to the decrease of the quantity of MnSi secondary phase, which reduces the thermoelectric proprieties.

In the milling experiments, using different process control agents (PCA) it is possible to control the MnSi phase. Hexane conducts to the formation of 38.8% of MnSi phase, acetone to 8.7% and ethanol to 5.3%. Milling without any PCA leads to the formation of 49.5% MnSi/HMS phase [10]. In order to obtain the proper HMS, the conditions can be summarized to be small milling time and high rotation speed according to [6, 13]. Prolonged milling conducts to the decomposition of HMS compound in MnSi phase as a result of the excess energy which is generated by collisions [14].

The increase in the thermoelectric properties can be achieved by doping. Adding Yb, the carrier concentration increases, and MnSi phase quantity decreases [14]. By doping with Co a homogenous microstructure is obtained and the ZT increases proportionally to the concentration of Co [12]. Other chemical elements that are studied for increasing the thermoelectric proprieties are Cr, Ti, Fe, Al, and Ge. The doping increases the thermoelectric proprieties only if the concentration of elements does not exceed the limit of solubility because the doped elements are located at Mn sites [15-18].

The present paper is focused on the synthesis of HMS with the chemical composition MnSi1.75. The formation of this compound by mechanical milling is studied as a function of the milling time. The paper presents the evolution of the powder morphology and the distribution of the chemical elements in the samples after milling. The thermal stability of powders is also presented and discussed.

Experimental

The thermoelectric material has been obtained starting from elemental powders of manganese with purity of 99.3% (-325 mesh, Alfa Aesar) and silicon with purity of 99.9% (-100 mesh, Alfa Aesar), in a stoichiometric ratio corresponding to $MnSi_{1.75}$ compound formula. The powder mixture was loaded into the vial with grinding media after the prior homogenisation of the elemental powders. The mechanical milling was made in a planetary ball mill Fritsch Pulverisette 6 using a ball to powder mass ratio (BPR) of 10:1, and a 400 rpm rotational speed of vial. The vial and balls are of stainless steel with a diameter of 14 mm. For the protection of powders which are subjected to milling process from oxidation, the milling was done under argon atmosphere. The milling was conducted up to 18 hours, and sampling was done after the following milling times: 0, 1, 2, 4, 6, 8, 10, 14 and 18 hours.

The structural study and phases composition of the samples were investigated by X-ray diffraction using an INEL 3000 Equinox diffractometer using Kα radiation of Co (λ = 1.79026 Å). To study the morphology of the powders and the local chemical homogeneity a JEOL- JSM 5600 LV electron microscope equipped with EDX spectrometer (Oxford Instruments, INCA 2000 soft) was used. The thermal stability of the samples was investigated by differential scanning calorimetry (DSC), using a LabSys-Setaram apparatus. The DSC investigations were performed in an argon atmosphere, up to 1000 °C, with heating/cooling rate of 10 °C/min using alumina as a reference sample. The presence of oxide inside the probe was investigated by the Fourier

Materials Research Proceedings **8** (2018) 88-88 doi: http://dx.doi.org/10.21741/9781945291999-9

Transform Infrared (FTIR) technique using Spectrum BX II apparatus. The experiment was realised by embedding the Mn-Si powder into the potassium bromide pellet.

Results and discussion

X-ray diffraction patterns of the mechanically milled powders are presented in Fig. 1. In diffraction pattern of the starting sample are identified the peaks corresponding to the used elemental powders. In the diffraction patterns corresponding to the sample milled for one hour is observed a reduction of the peaks intensity and a pronounced broadening. This is assigned to the reduction of crystallite size and an increase of the internal stresses [19]. The sample milled for 2 hours presents similar behavior. A new MnSi phase appears after 4 hours of milling. The formation of the HMS compound begins after 6 hours of mechanical milling. The complete reaction of the elements is observed after 18 hours.

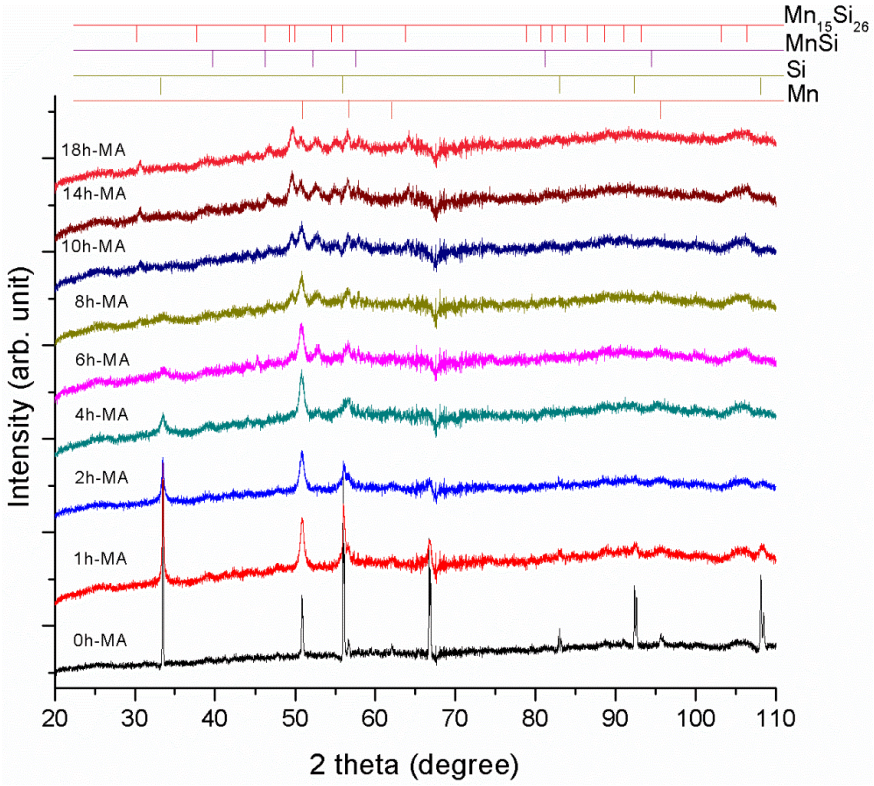

Fig. 1. X-ray diffraction of elemental powder mixture corresponding to chemical composition MnSi1.75 at different milling times.

The evolution of morphology and the distribution map of chemical elements was analyzed and is presented in Fig. 2. The SEM image presented in Fig. 2a is recorded on starting powders mixture. The particles present polyhedral irregular shapes. The distribution map for starting mixture reveals a good homogenisation of particles before loading in the vial for the milling process. A good homogenisation of powders is necessary to reduce as much as possible the silicon deposit on the balls, being more ductile than manganese, this can lead to the increase of the mechanical alloying duration as has been already reported in [20]. The image of powder milled for 4 hours (Figure 2 b), presents agglomeration of powder particles. After 4 hours of milling, manganese is more homogenously distributed as compared with the starting sample, due to initiation of the alloying process by milling. Powder milled 18 hours presents an irregular shape,

Materials Research Proceedings **8** (2018) 88-88 doi: http://dx.doi.org/10.21741/9781945291999-9

the dimension of the particles is small than 50 μm and much smaller as compared to particles of the starting sample. The sample milled for 18 hours shows particles with a size of less than 1 μm and particles with a size of a few micrometers that are composed of fine particles that are welded together. After 18 hours of mechanical milling, the distributions maps of manganese and silicon are uniform.

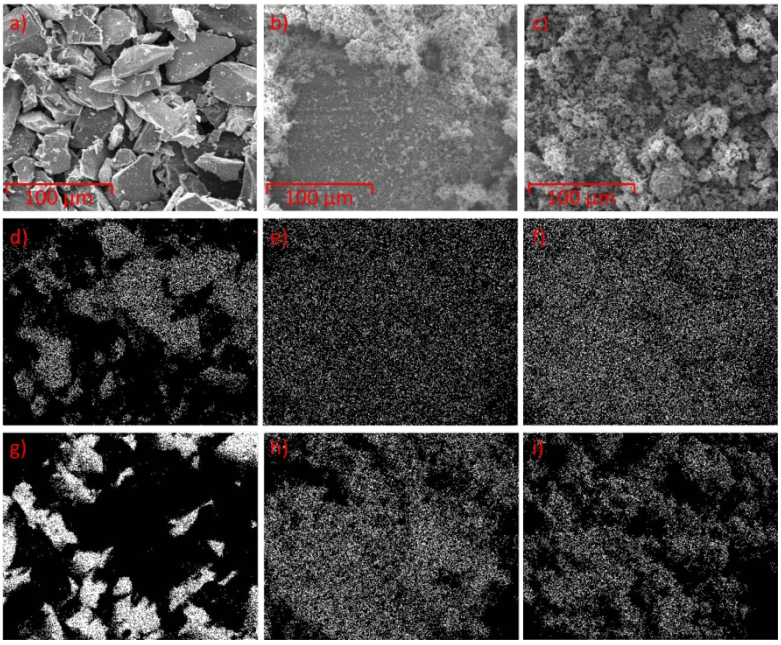

Fig. 2. SEM images for probe milled a) 0h; b) 4h; 18h. Map distribution of manganese is presented in d, e, f, and for silicon in g, h, i for initial mixture; and 4 hours; and respectively 18 hours.â

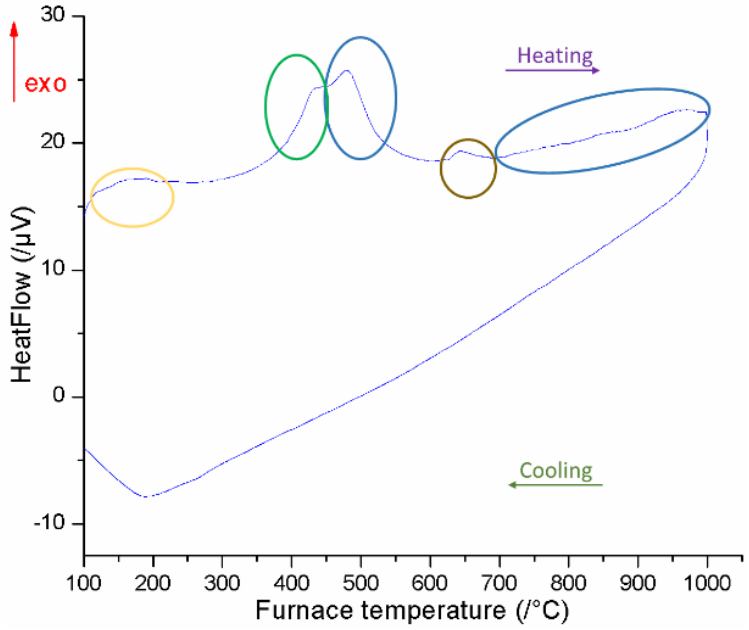

Fig. 3. DSC analysis of the sample milled for 4 hours. Heating was made up to 1000 ^{o}C with a heating rate of 10 ^{o}C / min.

Materials Research Proceedings **8** (2018) 88-88 doi: http://dx.doi.org/10.21741/9781945291999-9

DSC analyses of the sample milled for 4 hours is shown in Fig. 3. The DSC curve on heating up to 1000 ^{o}C present 5 distinct phenomena but the curve on cooling does not present any phenomena. To identify the phase transition after each event, X-ray diffraction was performed after DSC measurements at temperatures corresponding to each event up to 1000 °C. The X-ray diffraction is presented in Fig. 4. The first phenomenon is the stresses release of crystalline structure [21]. The stresses release peak is very broad and has the maximum around 200 °C. The second maximum corresponds to the formation of MnSi phase and has its maximum at 430 ^{o}C. The third thermal event corresponds to the formation of the $Mn_{15}Si_{26}$ chemical compound formation. The fourth and the fifth will be explained in the next section.

In the X-ray diffraction pattern corresponding to powders heat treated at 350 ^{o}C exhibits in comparison with the as-prepared sample only a peak narrowing. Annealing up to 450 ^{o}C conducts to the formation of MnSi phase and a small quantity of $Mn_{15}Si_{26}$ compound. In addition peaks of MnO are observed, indicating the sample oxidation. Heating up the sample at 550 ^{o}C, the formation of the $Mn_{15}Si_{26}$ compound is continued. Unfortunately, the oxidation of manganese continues as well, and the MnO further reacts and transforms into Mn_3O_4. By heating up to 700 ^{o}C there are no major changes in the samples, compared with the samples heated at 500 ^{o}C. While heating at 1000 ^{o}C major changes is recorded, the MnO peaks disappear being replaced by Mn_3O_4 peaks. The peaks corresponding to the MnSi phase and that of the $Mn_{15}Si_{26}$ compound grow in intensity and becomes narrower, as the crystallite mean size increases.

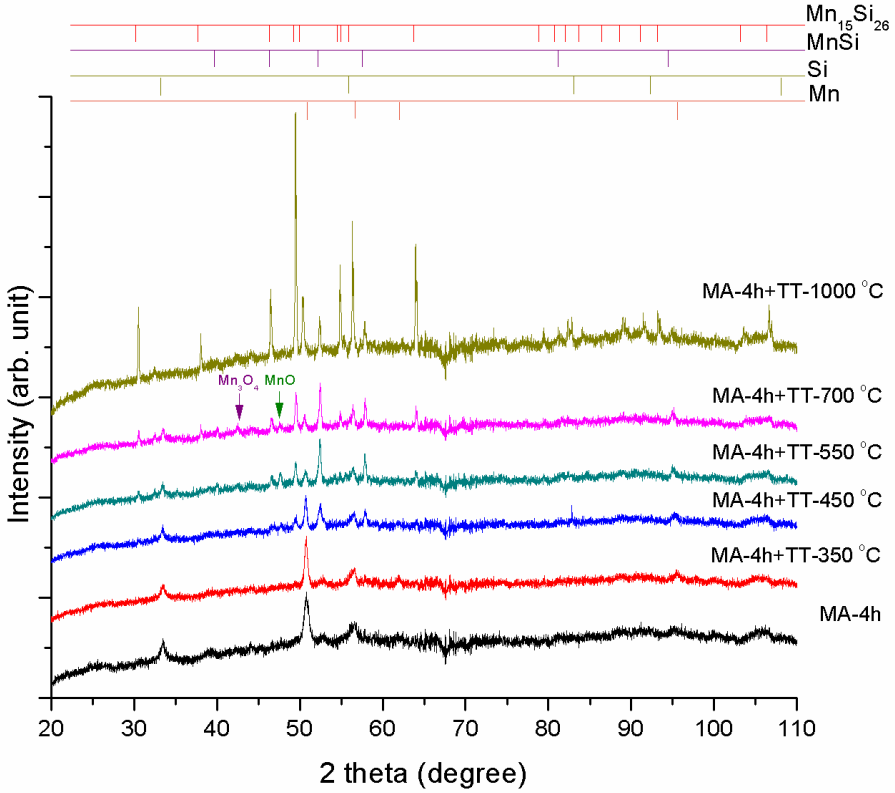

Fig. 4. X-ray diffraction patterns for the 4-hour mechanical alloyed sample and DSC at 350 ^{o}C, 450 ^{o}C, 550 ^{o}C, 700 ^{o}C and 1000 ^{o}C with a heating rate of 10 ^{o}C/min.

The oxidation of the samples can occur during sampling, that was performed in air and powders probably adsorbed oxygen from the atmosphere. To elucidate this assumption the samples were subjected to FTIR analyse. The result of FTIR analyze is presented in Fig. 5. In the FTIR

Materials Research Proceedings **8** (2018) 88-88 doi: http://dx.doi.org/10.21741/9781945291999-9

spectrum, several adsorption bands were recorded. It was recorded the adsorption band corresponding to the Mn-O stretching vibration at 655 cm^{-1} [22-25]. At 1029 cm^{-1} was recorded a wide abortion band, attributed to the stretching vibrations of Si-O-Si bond [22, 26], Si-OH [27], Mn-OH. The Mn-OH group has another maximum at 1422 cm^{-1} [28]. The next band, recorded at 1615 cm^{-1}, was attributed to the adsorbed hydroxyl groups (O-H bending mode) [23].

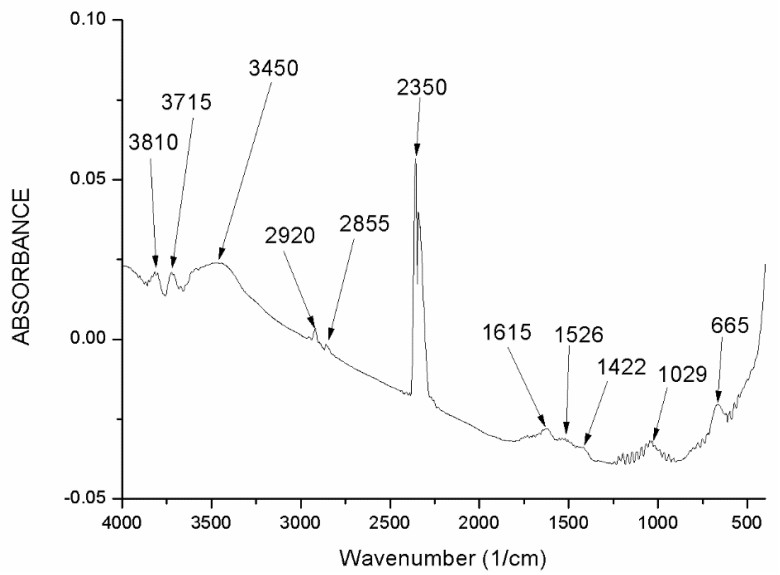

Fig. 5. FTIR spectra for $MnSi_{1.75}$ mechanical alloyed 18 hours.

The bands at 3810 cm^{-1} and 3715 cm^{-1} correspond to asymmetric stretch and symmetric stretch. This fact leads to the idea that molecular water exists in the probe [29]. The most intense maximum (2350 cm^{-1}) correspond to CO_2 [29, 30]. The absorption band in the range of 3400-3600 cm^{-1} corresponds to the O-H stretching vibration, the presence of O-H vibration is possible to appear because the powders absorb the water from the air [22,]. For the upcoming experiments, in order to avoid oxidation, the probes will be drawn in a controlled atmosphere.

Summary

From the preparation of Mn-Si alloy by mechanical milling route in the given condition the following conclusions can be drawn:

1. By solid state reaction of elemental powders, MnSi phase can be obtained, in the first stage, and the $Mn_{15}Si_{26}$ compound in the second stage.
2. The time required for complete reaction of the elements on the Fritsch Pulverisette 6 planetary mill with the selected parameters is 18 hours.
3. In the first hours of mechanical alloying, a fragmentation of manganese particles is observed, in which the most fragile component is.
4. After complete reaction, a powder of fine particle size is obtained.
5. The thermal treatment of the milled but unreacted powder leads to the complete reaction of the elements, but for the alloyed powder, the heat treatment only has the effect of increasing the grain size and stress release.

References

[1] M. S. Dresselhaus, G. Chen, M. Y. Tang, R. Yang, H. Lee, D. Wang, Z. Ren, J. P. Fleurial, P. Gogna, New directions for low-dimensional thermoelectric materials, Adv. Mater. 19 (2007) 1043–1053. https://doi.org/10.1002/adma.200600527

[2] Z. Du, T. Zhu, X. Zhao, Enhanced thermoelectric properties of $Mg_2Si_{0.58}Sn_{0.42}$ compounds by Bi doping, Mater. Letter. 66 (2012) 76–78. https://doi.org/10.1016/j.matlet.2011.08.031

[3] T. Yamada, Y. Miyazaki, H. Yamane, Preparation of Higher Manganese Silicide (HMS) bulk and Fe-containing HMS bulk using a Na–Si melt and their thermoelectrical properties, Thin Solid Films 519 (2011) 8524–8527. https://doi.org/10.1016/j.tsf.2011.05.032

[4] X. Hu, D. Mayson, M. R. Barnett, Synthesis of Mg_2Si for thermoelectric applications using magnesium alloy and spark plasma sintering, J All. Compd. 589 (2014) 485–490. https://doi.org/10.1016/j.jallcom.2013.11.092

[5] X. Chen, L. Shi, J. Zhou, J. B. Goodenough, Effects of ball milling on microstructures and thermoelectric properties of higher manganese silicides, J All. Compd. 641 (2015) 30–36. https://doi.org/10.1016/j.jallcom.2015.04.048

[6] Z. Zamanipoura, X. Shia, M. Mozafari, J. S. Krasinski, L. Tayebib, D. Vashaee, Synthesis, characterization, and thermoelectric properties of nanostructured bulk p-type $MnSi_{1.73}$, $MnSi_{1.75}$, and $MnSi_{1.77}$, Ceram. Int. 39 (2013) 2353–2358. https://doi.org/10.1016/j.ceramint.2012.08.086

[7] D. B. Migas, V. L. Shaposhnikov, A. B. Filonov, and V. E. Borisenko, Ab initio study of the band structures of different phases of higher manganese silicides, Phys. Rev. B 77 (2008) 075205. https://doi.org/10.1103/PhysRevB.77.075205

[8] H. Lee, G. Kim, B. Lee, J. Kim, S. M. Choi, K. H. Lee, W. Lee, Effect of Si content on the thermoelectric transport properties of Ge-doped higher manganese silicides, Scripta Mater. 135 (2017) 72–75. https://doi.org/10.1016/j.scriptamat.2017.03.011

[9] A.J. Zhou, X.B. Zhao, T.J. Zhu, Y.Q. Cao, C. Stiewe, R. Hassdorf, E. Mueller, Composites of higher manganese silicides and nanostructured secondary phases and their thermoelectric properties, J Electron Mater. 38 (2009) 1072-1077. https://doi.org/10.1007/s11664-009-0774-7

[10] A.J. Zhou, X.B. Zhao, T.J. Zhu, T. Dasgupta, C. Stiewe, R. Hassdorf, E. Mueller, Mechanochemical decomposition of higher manganese silicides in the ball milling process, Intermetallics 18 (2010) 2051-2056. https://doi.org/10.1016/j.intermet.2010.06.008

[11] D.Y.N. Truong, H. Kleinke, F. Gascoin, Preparation of pure Higher Manganese Silicides through wet ball milling and reactive sintering with enhanced thermoelectric properties, Intermetallics 66 (2015) 127-132. https://doi.org/10.1016/j.intermet.2015.07.002

[12] T. Itoh, S. Uebayashi, Cobalt an iron doping effect on thermo-electric properties of higher manganese silicides prepared by mechanical milling and pulse discharge sintering, J Jpn. Soc. Powder Powder Metall. 63 (2016) 491-496. https://doi.org/10.2497/jjspm.63.491

[13] D. K. Shin, K. W. Jang, S. C. Ur, I. H. Kim, Thermoelectric properties of higher manganese silicides prepared by mechanical alloying and hot pressing, J Electron Mater. 42 (2013) 1756-1761. https://doi.org/10.1007/s11664-012-2415-9

[14] M. Saleemi, A. Famengo, S. Fiameni, S. Boldrini, S. Battiston, M. Johnsson, M. Muhammed, M.S. Toprak, Thermoelectric performance of higher manganese silicide nanocomposites Journal of Alloys and Compounds 619 (2015) 31–37. https://doi.org/10.1016/j.jallcom.2014.09.016

[15] V. Ponnambalam, D. T. Morelli, S. Bhattacharya, T. M. Tritt The role of simultaneous substitution of Cr and Ru on the thermoelectric properties of defect manganese silicides $MnSi_{\delta}$ ($1.73 < \delta < 1.75$), J All. Compd. 580 (2013) 598–603. https://doi.org/10.1016/j.jallcom.2013.07.136

[16] L.D. Ivanova, Preparation of thermoelectric materials based on higher manganese silicide, Inorganic Mater. 47 (2011) 965–970. https://doi.org/10.1134/S002016851109010X

[17] W. Luo, H. Li, F. Fu, W. Hao, X. Tang Improved thermoelectric properties of Al-doped higher manganese silicide prepared by a rapid solidification method, J. Electron. Mater. 40 (2011) 1233-1237. https://doi.org/10.1007/s11664-011-1612-2

[18] A.J. Zhou, T.J. Zhu, X.B. Zhao, S.H. Yang, T. Dasgupta, C. Stiewe, R. Hassdorf, E. Mueller, Improved thermoelectric performance of Higher Manganese Silicides with Ge additions J. Electron. Mater. 39 (2010) 2002-2007. https://doi.org/10.1007/s11664-009-1034-6

[19] T.F. Marinca, H.F. Chicinas, B.V. Neamt, O. Isnard, P. Pascuta, N. Lupu, G. Stoian, I. Chicinaș, Mechanosynthesis, structural, thermal and magnetic characteristics of oleic acid coated Fe_3O_4 nanoparticles, Mater. Chem. Phys. 171 (2016) 336-345. https://doi.org/10.1016/j.matchemphys.2016.01.025

[20] T. Itoh, M. Yamada, Synthesis of thermoelectric Manganese Silicide by mechanical alloying and pulse discharge sintering J. Electron. Mater. 38 (2009) 925-929. https://doi.org/10.1007/s11664-009-0697-3

[21] T.F. Marinca, B.V. Neamtu, F. Popa, V.F. Tarta, P. Pascuta, A.F. Takacs, I. Chicinas, Synthesis and characterization of the $NiFe_2O_4/Ni_3Fe$ nanocomposite powder and compacts obtained by mechanical milling and spark plasma sintering, Appl. Surf. Sci. 285P (2013) 2-9. https://doi.org/10.1016/j.apsusc.2013.07.145

[22] A. Belhadi, L. Boudjellal, S. Boumaza, M. Trari. Hydrogen production over the hetero-junction MnO_2/SiO_2. Int. J Hydrogen Energy 43 (2017) 3418-3423. https://doi.org/10.1016/j.ijhydene.2017.06.086

[23] T. K. Ghorai, S. Pramanik, P. Pramanik, Synthesis and photocatalytic oxidation of different organic dyes by using Mn_2O_3/TiO_2 solid solution and visible light, Appl. Surf. Sci. 255 (2009) 9026–9031. https://doi.org/10.1016/j.apsusc.2009.06.086

[24] X. Yang, L. Zhao, L. Zheng, M. Xu, X. Cai, Polyglycerol grafting and RGD peptide conjugation on MnO nanoclusters for enhanced colloidal stability, selective cellular uptakeand cytotoxicity, Colloids and Surfaces B: Biointerfaces 163 (2018) 167–174. https://doi.org/10.1016/j.colsurfb.2017.12.034

[25] M. Zheng, H. Zhang, X. Gong, R. Xu, Y. Xiao, H. Dong, X. Liu, Y. Liu, A simple additive-free approach for the synthesis of uniform manganese monoxide nanorods with large specific surface area, Nanoscale Res. Lett. 1 (2013), 166. https://doi.org/10.1186/1556-276X-8-166

[26] G. Nuyts, S.e Cagno, K. Hellemans, G. Veronesi, M. Cotte, K. Janssens, Study of the early stages of Mn intrusion in corroded glass by means of combined SR FTIR/μXRF imaging and XANES spectroscopy, Procedia Chem. 8 (2013) 239-247. https://doi.org/10.1016/j.proche.2013.03.030

[27] M. Abdelmouleh, S. Boufi, M.N. Belgacem, A.P. Duarte, A. Ben Salah, A. Gandini, Modification of cellulosic fibres with functionalised silanes: development of surface properties Int. J. Adhes. Adhes. 24 (2004) 43–54. https://doi.org/10.1016/S0143-7496(03)00099-X

[28] S. A. Moon, B. K. Salunke, B. Alkotaini, E. Sathiyamoorthi, B. S. Kim, Biological synthesis of manganese dioxide nanoparticles by Kalopanax pictus plant extract IET, Nanobiotechnol. 9 (2015) 220-225. https://doi.org/10.1049/iet-nbt.2014.0051

[29] W. Laminack, J. L. Gole, M. G. White, S. Ozdemir, A. G. Ogden, H. J. Martin, Z. Fang, T. H. Wang, D. A. Dixon, Synthesis of nanoscale silicon oxide oxidation state distributions: The transformation from hydrophilicity to hydrophobicity, Chem. Phys. Lett. 653 (2016) 137–143. https://doi.org/10.1016/j.cplett.2016.04.079

[30] B.V. Neamtu, O. Isnard, I. Chicinas, C. Vagner, N. Jumate, P. Plaindoux, Influence of benzene on the Ni_3Fe nanocrystalline compound formation by wet mechanical alloying: An investigation combining DSC, X-ray diffraction, mass and IR spectrometries, Mater. Chem. Phys. 125 (2011) 364–369. https://doi.org/10.1016/j.matchemphys.2010.10.056

[31] Y. Xu, H. Lin, Y. Li, H. Zhang The mechanism and efficiency of MnO2 activated persulfate process coupled with electrolysis Science of the Total Environment 609 (2017) 644–654. https://doi.org/10.1016/j.scitotenv.2017.07.151